NASA Technical Paper 1891

Correlation of Ideal and Actual Shear Strengths of Metals With Their Friction Properties

Kazuhisa Miyoshi and Donald H. Buckley

JULY 1981

NASA

NASA Technical Paper 1891

Correlation of Ideal and Actual Shear Strengths of Metals With Their Friction Properties

Kazuhisa Miyoshi and Donald H. Buckley
Lewis Research Center
Cleveland, Ohio

National Aeronautics
and Space Administration

**Scientific and Technical
Information Branch**

1981

Summary

An investigation was conducted to define the relation between the ideal and actual shear strength of clean metals and their friction properties when in contact with clean diamond, boron nitride, silicon carbide, manganese-zinc ferrite, and the metals themselves.

Estimates for the ideal shear strength for metals were obtained from the shear modulus, the repeat distance of atoms in the direction of shear in metal, and the interplanar spacing of the shearing planes.

The coefficient of friction for metals is related to both ideal and actual shear strength of metals. The results of this investigation indicate that the higher the strength of the metal, the lower the coefficient of friction.

Introduction

A clean metal in sliding contact with a clean nonmetal or the metal itself will fail either in tension or in shear because some of the interfacial bonds are generally stronger than the cohesive bonds in the cohesively weaker metal. The failed metal subsequently transfers to nonmetallic material or the other contacting metal (see fig. 1 and refs. 1 to 5). It is, therefore, anticipated that friction, metal transfer, and metal wear would be related to chemical, physical, and metallurgical properties and to the strength of metals. For example, the effect of chemical properties (such as affinity or activity) of the metal has been observed to play an important role in the friction, metal transfer, and form of metal wear debris, which is generated by the fracture of cohesive bonds (refs. 1 to 5). In general, the less active the metal, the lower the coefficient of friction and the less transfer to the nonmetallic material.

The present authors have also investigated the relation between the ideal tensile strength and the friction properties of metals (ref. 6). It was found that the coefficient of friction decreased with increasing values of the ideal tensile strength.

The objective of this paper is to discuss the relations between the ideal and actual shear strengths and the friction properties of metals in contact with metals and nonmetals. The ideal shear strength τ_{max} of a solid subjected to a simple shear mode of deformation is estimated (ref. 7). The actual shear strengths for the metals are taken from the data of Bridgman (ref. 8).

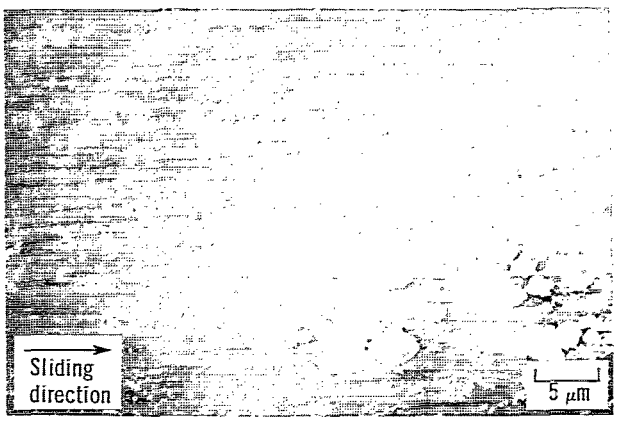

(a) Wear track showing transfer of iron to single-crystal silicon carbide.

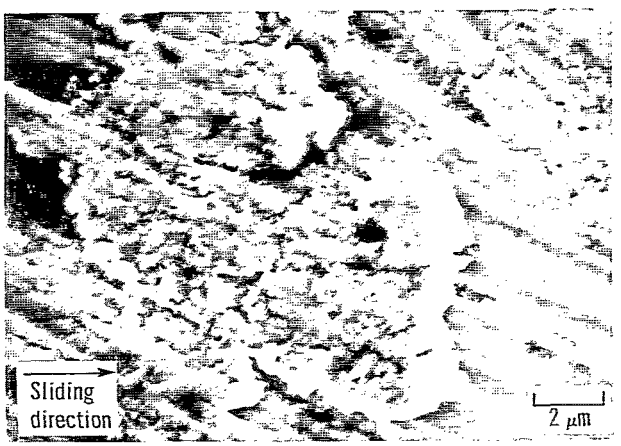

(b) Wear scar of iron.

Figure 1. - Scanning electron micrographs of wear track on the silicon carbide surface and wear scar of iron as a result of single pass of rider in vacuum. Silicon carbide {0001} surface; sliding direction <10$\bar{1}$0>; sliding velocity 3 mm/min; load, 0.2 N; room temperature; vacuum pressure, 10^{-8} Pa.

The nonmetals examined included single-crystal diamond, pyrolytic boron nitride, single-crystal silicon carbide, and single-crystal manganese-zinc ferrite.

All sliding friction experiments were conducted with light loads of 0.01 to 0.5 newton, at a sliding

velocity of 0.70, 0.77, or 3 millimeters per minute, in a vacuum of 10^{-8} pascal and at room temperature. Experiments were conducted in this investigation with the metal pin specimens sliding on the nonmetal or metal flats. The radius of pin specimens was 0.79 millimeter.

Symbols

b	repeat distance of atoms in the direction of shear
d	interplanar spacing of shearing planes
E	Young's modulus
$\overline{F}_{max}$	average friction force
G	shear modulus
k	constant
W	normal load
x	displacement of the shear plane from its neighbors
γ	surface energy per unit area
μ	coefficient of friction
σ_{max}	ideal tensile strength
τ_{max}	ideal shear strength

Materials

Diamond. – Natural, single-crystal diamonds were used in these experiments. The {111} plane was parallel to the sliding interface. The specimens that were less than $\pm 2^\circ$ of the low index {111} plane were used. The samples were in the form of flat platelets and had a mean surface area of about 30 square millimeters.

Pyrolytic boron nitride. – The boron nitride was 99.99 percent pure compound of boron and nitrogen. It has a hexagonal crystal structure with a $c/2$ layer spacing of 0.233 to 0.343 nanometer and a nearest neighbor spacing of 0.146 nanometer in the hexagonal lattice. The c direction was perpendicular to the sliding interface with the basal planes therefore parallel to the interface.

Silicon carbide. – The single-crystal silicon carbide platelets used were a 99.9 percent pure compound of silicon and carbon. Silicon carbide has a hexagonal close-packed crystal structure. The basal plane was paralled to the interface.

Manganese-zinc ferrite. – The single-crystal manganese-zinc ferrite platelets were 99.9 percent pure oxide. The crystal is that of spinels in which the oxygen ions are in a nearly close-packed cubic array. The {110} plane was parallel to the interface.

Metals. – Two groups of metals were used. One was all single crystals, and the other was all polycrystalline. The single-crystal metals are used for the sliding friction experiments with pyrolytic boron nitride and with the metals themselves. The body-centered-cubic metals had the {110} plane on their surface and, therefore, parallel to the sliding interface. The face-centered-cubic metals had the {111} planes parallel to the sliding interface and the hexagonal metals had the {0001} surfaces parallel to that interface.

The polycrystalline metals are used for the experiments with diamond, silicon carbide, and manganese-zinc ferrite.

The titanium was 99.97 percent pure; the copper was 99.999 percent pure; and all the other metals were 99.99 percent pure in the single-crystal and polycrystalline forms.

Apparatus

The apparatus used in the investigation was mounted in an ultrahigh vacuum system. The apparatus is capable of measuring adhesion, load, and friction. The vacuum system also contained an Auger emission spectrometer system (AES) for surface analysis. The mechanism used for measuring adhesion, load, and friction is shown schematically in figure 2. A gimbal-mounted beam is projected into the vacuum system. The beam contains two flats machined normal to each other with strain gages mounted thereon. The metal pin is mounted on the end of the beam. As a load is applied by moving the beam normal to the disk, it is measured by the strain gage. The vertical sliding motion of the pin along the disk surface is accomplished through a motorized gimbal assembly. Under an applied load the friction

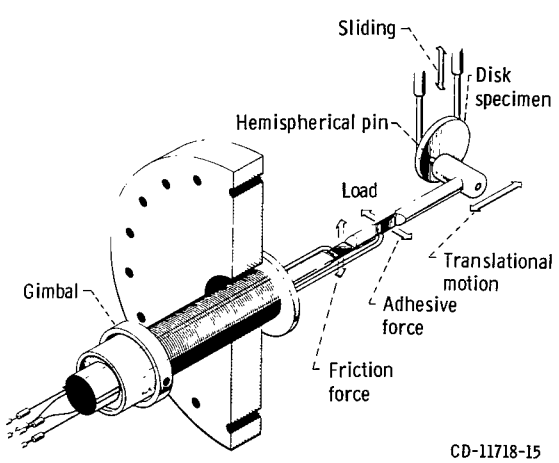

Figure 2. - High-vacuum friction and wear apparatus.

force is measured during vertical translation by the strain gage mounted normal to that used to measure load. This feature was used to examine the coefficient of friction at various loads (as shown in fig. 2). Multiple wear tracks could be generated on the disk surface by the translating motion of the beam containing the pin.

Experimental Procedure

The disk flat and metal pin specimens were polished with a diamond powder (particle diameter, 3 μm) and with an aluminum oxide (Al_2O_3) powder (1 μm). The radius of the pins was 0.79 millimeter. The disk and pin surfaces were rinsed with 200-proof ethyl alcohol.

The specimens were placed in the vacuum chamber, and the system was evacuated and subsequently baked out to obtain a pressure of 1.33×10^{-8} pascal (10^{-10} torr). When this pressure was obtained, argon gas was bled back into the vacuum chamber to a pressure of 1.3 pascals. A 1000-volt-direct-current potential was applied, and the specimens (both disk and rider) were obtained to determine the degree of surface cleanliness. When the desired degree of cleanliness of the disk was achieved, friction experiments were conducted.

Loads up to 0.5 newton were applied to the pin-disk contact by deflecting the beam of figure 2. Both load and friction force were continuously monitored during a friction experiment. Sliding velocity was 0.70, 0.77, and 3 millimeter per minute. All friction experiments in vacuum were conducted with the system evacuated to a pressure of 10^{-8} pascal.

A friction trace is generally characterized by a stick-slip behavior. The coefficient of friction μ is defined as $\mu = F_{max}/W$, where F_{max} is the average friction force calculated from maximum peak heights in the observed friction force trace and W is the normal load.

Theoretical Strength of Solids

The generally accepted thinking with respect to fracture of solids is that of the ideal elastic solid or one which exhibits elastic response to a load until such time as atomic separation takes place on a plane by overcoming the interatomic forces. At the atomistic level fracture occurs when bonds between atoms are broken across a fracture plane and a new surface is created. This can occur by breaking bonds perpendicular to the fracture plane (fig. 3(a)) or by shearing bonds across the fracture plane (fig. 3(b)). Such behavior is expected in the case of an ideal

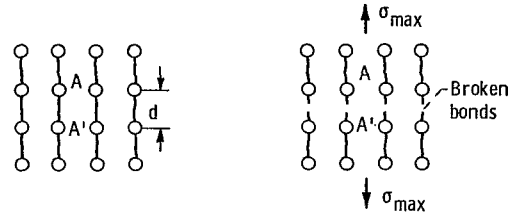

(a) Tensile fracture.

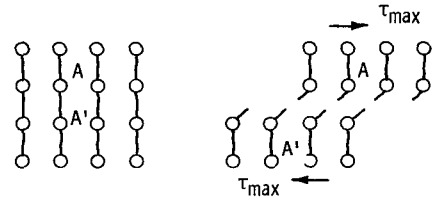

(b) Shear fracture.

Figure 3. - Fracture viewed at atomistic level in terms of breaking of atomic bonds.

crystalline solid which contains no defects of any kind. At this level the fracture criteria are simple; fracture occurs when the local stress builds up either to the theoretical cohesive strength or to the theoretical shear strength. The theoretical cohesive strength has already been discussed in reference 6.

The calculation of the theoretical cohesive strength of an ideal elastic solid is based on the proposition that all the energy of separation is available for the creation of two new surfaces; the only expenditure in creating these two surfaces is assumed to be the surface energy. If the atoms A and A′ in figure 3(a) are pulled apart, the stress required to separate the plane is the theoretical strength σ_{max} and when that is reached, the bonds are broken. The theoretical strength (the ideal uniaxial tensile strength) is then given by well-known equation,

$$\sigma_{max} = \sqrt{\frac{E\gamma}{d}} \tag{1}$$

where E is the appropriate Young's modulus, γ is the surface energy per unit area, and d is the interplanar spacing of the planes perpendicular to the tensile axis (refs. 7 or 9 to 12). In the equation the ideal strength of solid is directly related to other macroscopic physical properties. The foregoing approach is equally applicable to any solid. Frenkel used a similar method to estimate the ideal shear strength τ_{max} of a solid subjected to a simple shear mode of deformation (ref. 7 or 13). It is assumed that, for any solid, the shear stress to shear any plane a distance x over its neighbor was given by

$$\tau = k \sin \frac{2\pi x}{b} \tag{2}$$

where b is the appropriate repeat distance in the direction of shear (the planes are assumed to be undistorted by the shear) and K is chosen to give the correct shear modulus G. It is then easily shown that

$$\tau_{max} = \frac{Gb}{2\pi d} \quad (3)$$

where d is the interplanar spacing of the shearing planes.

The ideal strength of metals, based on atomic forces, is of the order of 100 to 1000 times greater than that observed. The various reasons for this discrepancy between ideal and observed strength are discussed in detail, but the more important ones are (1) lattice imperfections, (2) crystalline anisotropy, and (3) the ability of metals to deform by shear.

As greater and greater mechanical strengths are obtained from engineering materials, it is only logical to ask, What is the upper limit to the strength of a solid? This upper limit or maximum strength has come to be referred to as the ideal strength.

Survey of Physical Properties

The shear modulus is also known as the torsion modulus or modulus of rigidity. The values of the shear moduli for bulk, polycrystalline materials are listed in table I (ref. 14). The shear modulus, like Young's modulus, has a marked dependence on the electronic configuration of the element (ref. 14). Table I also lists lattice constants of metals (refs. 15 and 16). The values of the lattice constants are used for the estimations of an interplanar spacing of slip plane and an atomic spacing in the direction of shear. Generally, the slip plane is the plane of the greatest atomic density, and the slip direction is the closest packed direction in that plane. The experimental results of slip systems at room temperature are given in table II (ref. 17).

The general rule related to slip systems is obeyed in the case of face-centered-cubic structure. In the body-centered-cubic structure there is general agreement that the slip direction is ⟨111⟩, which is the closest packed direction in this structure, but there is a lack of agreement with respect to the slip plane. Various planes have been reported, as indicated in table II. The geometry of the body-centered cubic lattice is such that for many orientations the maximum shear stress will act along the planes or combination of planes of the type {110}, {112}, or {123}. In the close-packed hexagonal structures both basal and nonbasal planes have a common slip direction ⟨1120⟩. Table III gives distances between planes in three crystallographic structures.

TABLE I. - SHEAR MODULUS AND LATTICE CONSTANTS

Metal	Shear modulus, GPa	Lattice constants, nm	
		a	c
Al	27	0.405	-----
Ni	75	.352	-----
Cu	45	.361	-----
Rh	150	.380	-----
Pd	51	.388	-----
Ir	210	.384	-----
Pt	61	.393	-----
V	47	0.304	-----
Cr	117	.288	-----
Fe	81	.287	-----
Nb	37	.330	-----
Mo	116	.314	-----
Ta	69	.330	-----
W	150	.316	-----
Ti	39	0.295	0.468
Co	76	.251	.407
Y	26	.365	.573
Zr	34	.323	.515
Ru	160	.270	.428
Re	180	.276	.446

Correlation of Friction with the Ideal Shear Strength

From equation (3) the values of the ideal shear strength were obtained and these are presented in table IV. It is assumed that the slip occurred on the slip plane in the slip direction, as indicated in table IV.

Figure 4 presents the coefficients of friction as a function of the ideal shear strength. The coefficient of friction data for various clean metals in contact with clean diamond, pyrolytic boron nitride, silicon carbide, manganese-zinc ferrite and metals themselves were used from the references 1 to 5. These figures indicate a decrease in friction with an increase of the ideal shear strength of the metal bond.

The ideal shear strength generally produces a correlation with the coefficients of friction for metals in contact with nonmetals, such as diamond, pyrolytic boron nitride, silicon carbide, and

TABLE II. - SLIP SYSTEMS AT ROOM TEMPERATURE

Metal	Slip systems	
	Directions	Planes
Al	$\langle 110 \rangle$	$\{111\}$
Ni		
Cu		
Rh		
Pd		
Ir		
Pt		
V	$\langle 111 \rangle$	$\{110\}$
Cr		$\{112\}$
Fe		$\{123\}$
Nb		
Mo		
Ta		
W		
Ti	$\langle 11\bar{2}0 \rangle$,	$\{0001\}$
Co	$\langle 11\bar{2}3 \rangle$	$\{10\bar{1}0\}$
Y		$\{10\bar{1}1\}$
Zr		$\{11\bar{2}2\}$
Ru		
Re		

TABLE III. - DISTANCES BETWEEN PLANES

Structure	Plane	Distances between planes
fcc	Octahedral $\{111\}$	$a_0{}^*/\sqrt{3}$
	Cubic $\{100\}$	$a_0/2$
	Dodecahedral $\{110\}$	$a_0/2\sqrt{2}$
bcc	Dodecahedral $\{110\}$	$\sqrt{2}\, a_0/2$
	Cubic $\{100\}$	$a_0/2$
	Octahedral $\{111\}$	$a_0/2\sqrt{3}$
Hexagonal	Basal $\{0001\}$	$c^\dagger$
	Prismatic $\{10\bar{1}0\}$	$a\sqrt{3}^\dagger/2$
	Pyramidal $\{10\bar{1}1\}$	$ac\sqrt{3}/\sqrt{3a^2 + 4c^2}$
	Prismatic $\{11\bar{2}0\}$	a

*a_0 is lattice constant of the cubic (fcc and bcc) structures.

†a and c are lattice constants of the hexagonal structure.

manganese-zinc ferrite, as shown in figure 4. The coefficients of friction for metals in contact with themselves are correlated with the shear strength, except for platinum and palladium, as shown in figure 4(e). In these figures the values of the shear strength for face-centered cubic metals are used from the results shown in table IV.

The shear strength values for the body-centered cubic metals are average values calculated from the values of the shear strength for three dominant slip systems. Those for the hexagonal metals are average values calculated from the values of the shear strength for two dominant slip systems, that is, $\{10\bar{1}0\}\langle 11\bar{2}0\rangle$ and $\{0001\}\langle 11\bar{2}0\rangle$.

Thus, the tensile and shear properties play important roles in the adhesion and friction of metals contacting nonmetals or metals contacting themselves. These simple calculations of the ideal strength and the correlation between the friction and the strength can be criticized on a variety of grounds. The extent of slip in a crystal depends on the magnitude of the shearing stresses produced by the applied forces and the orientation of the crystal with respect to these applied forces. This variation can be rationalized by the concept of the crystal's resolved shear stress for slip. Despite the foregoing the results of the relation between the coefficient of friction and the ideal strength may lead in turn to an appreciation for the role of the physical properties of materials in determining the tribological properties and the mechanical behavior of metals.

A good correlation between the coefficients of friction and the shear modulus (refer to table IV) was also found with metals contacting nonmetals. The correlations are very similar to those between the coefficient of friction and the shear strength, as shown in figure 4. This is to be expected at least for face-centered cubic and close-packed hexagonal metals because, as shown in table IV, the ratios of τ_{max} to G are essentially constant at a value of about 0.1. With the body centered cubic metals the ratio of τ_{max}/G is essentially constant at a value of about 0.6.

Correlation of Friction with the Actual Shear Strength

The theoretical shear strength as well as the theoretical tensile strength are much greater than the values commonly found experimentally (ref. 6).

In the former section and reference 6 the relations between the theoretical strengths and the friction properties of metals in contact with nonmetals and the metals themselves were discussed. There is, however, an obvious need to compare the actual strength of metals observed with the friction properties.

TABLE IV. - SIMPLE CALCULATIONS OF THE IDEAL SHEAR STRENGTH

(a) Face-centered cubic structure; shear plane and direction, $\{111\}\langle 110\rangle$

Metal	Shear strength, τ_{max}, GPa	Strength to modulus ratio, τ_{max}/G
Al	2.6	0.096 - 0.098
Ni	7.3	↓
Cu	4.4	↓
Rh	15	↓
Pd	5.0	↓
Ir	21	↓
Pt	5.9	↓

(b) Body-centered cubic structure

Metal	Shear plane and direction					
	$\{110\}\langle 111\rangle$		$\{112\}\langle 111\rangle$		$\{123\}\langle 111\rangle$	
	τ_{max}, GPa	τ_{max}/G	τ_{max}, GPa	τ_{max}/G	τ_{max}, GPa	τ_{max}/G
V	3.1	0.065 - 0.66	5.3	0.11	8.1	0.17
Cr	7.6	↓	13	↓	20	↓
Fe	5.3	↓	9.2	↓	14	↓
Nb	2.4	↓	4.2	↓	6.4	↓
Mo	7.5	↓	13	↓	20	↓
Ta	4.5	↓	7.8	↓	12	↓
W	9.8	↓	17	↓	26	↓

(c) Hexagonal structure

Metal	Shear plane and direction					
	$\{0001\}\langle 11\bar{2}0\rangle$		$\{10\bar{1}0\}\langle 11\bar{2}0\rangle$		$\{10\bar{1}1\}\langle 11\bar{2}0\rangle$	
	τ_{max}, GPa	τ_{max}/G	τ_{max}, GPa	τ_{max}/G	τ_{max}, GPa	τ_{max}/G
Ti	3.9	0.098 - 0.10	7.2	0.18 - 0.19	8.2	0.21
Co	7.5	↓	14	↓	16	↓
Y	2.6	↓	4.8	↓	5.5	↓
Zr	3.4	↓	6.3	↓	7.1	↓
Ru	16	↓	29	↓	34	↓
Re	18	↓	33	↓	38	↓

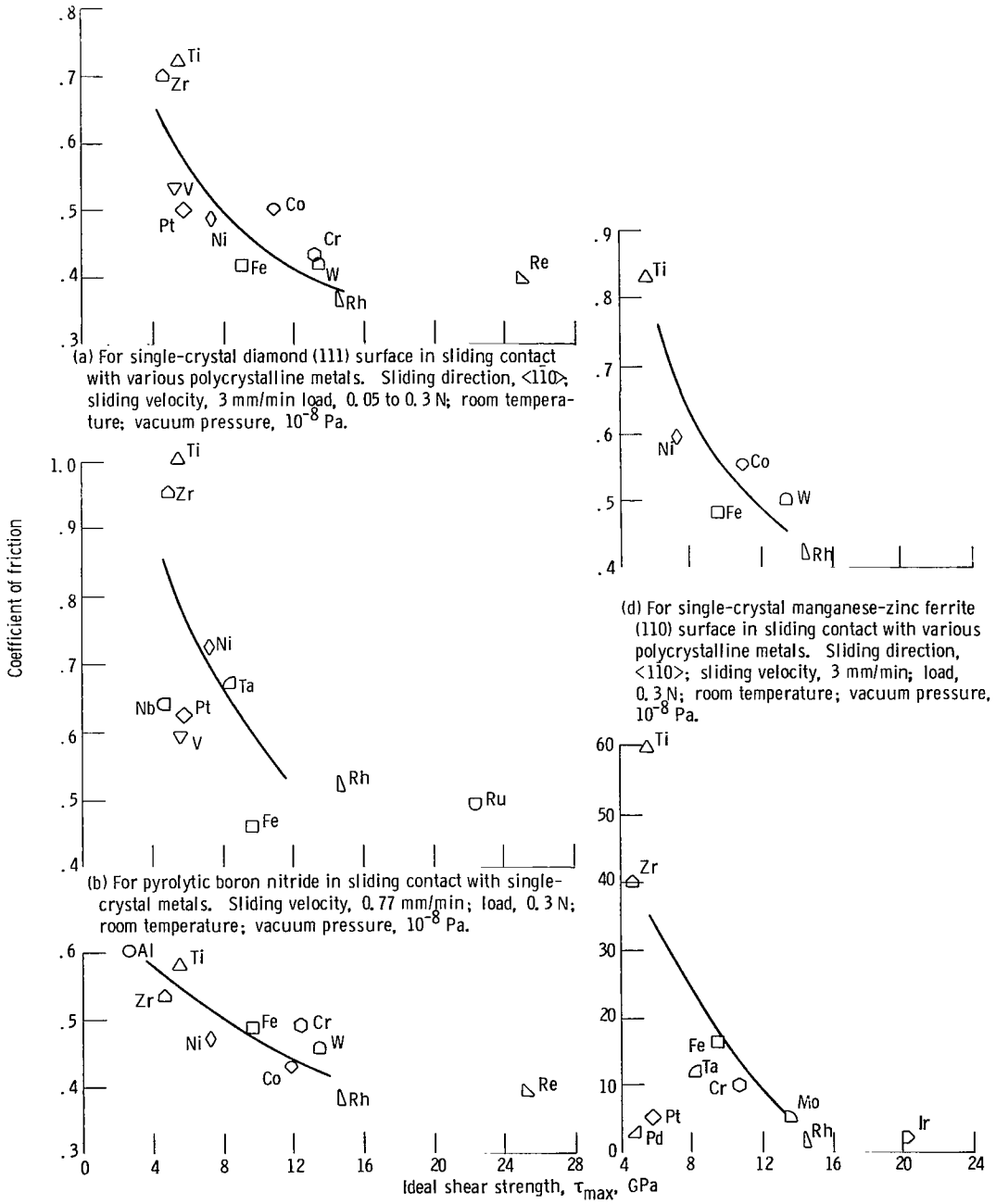

(a) For single-crystal diamond (111) surface in sliding contact with various polycrystalline metals. Sliding direction, <1$\bar{1}$0>; sliding velocity, 3 mm/min load, 0.05 to 0.3 N; room temperature; vacuum pressure, 10^{-8} Pa.

(b) For pyrolytic boron nitride in sliding contact with single-crystal metals. Sliding velocity, 0.77 mm/min; load, 0.3 N; room temperature; vacuum pressure, 10^{-8} Pa.

(c) For single-crystal silicon carbide (0001) surface in sliding contact with various polycrystalline metals. Sliding direction, <10$\bar{1}$0>; sliding velocity, 3 mm/min; load, 0.05 to 0.5 N; room temperature; vacuum pressure, 10^{-8} Pa.

(d) For single-crystal manganese-zinc ferrite (110) surface in sliding contact with various polycrystalline metals. Sliding direction, <1$\bar{1}$0>; sliding velocity, 3 mm/min; load, 0.3 N; room temperature; vacuum pressure, 10^{-8} Pa.

(e) For various single-crystal metals in sliding contact with themselves. Sliding velocity, 0.7 mm/min; load, 0.01 N; room temperature; vacuum pressure, 10^{-8} Pa.

Figure 4. - Coefficients of friction as function of the ideal shear strength of metals.

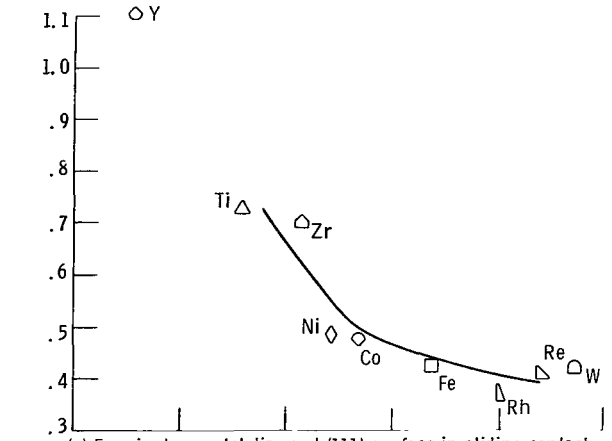

(a) For single-crystal diamond (111) surface in sliding contact with various polycrystalline metals. Sliding direction, $\langle 1\bar{1}0 \rangle$; sliding velocity, 3 mm/min; load, 0.05 to 0.3 N; room temperature; vacuum pressure, 10^{-8} Pa.

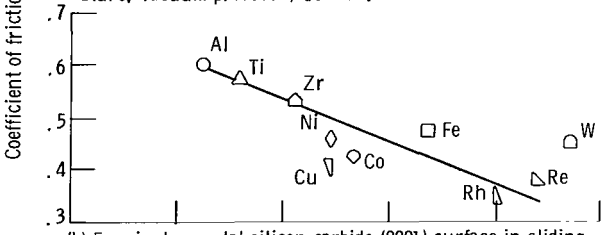

(b) For single-crystal silicon carbide (0001) surface in sliding contact with various polycrystalline metals. Sliding direction, $\langle 0\bar{1}0 \rangle$; sliding velocity, 3 mm/min; load, 0.05 to 0.5 N; room temperature; vacuum pressure, 10^{-8} Pa.

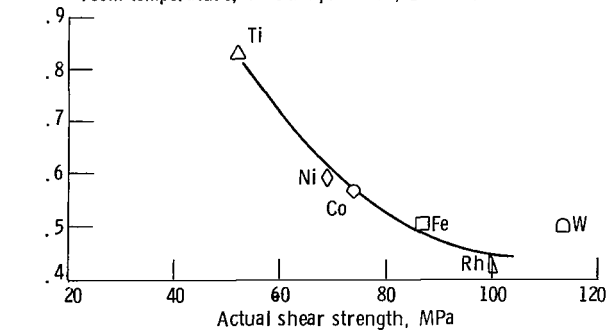

(c) For single-crystal manganese-zinc ferrite (110) surface in sliding contact with various polycrystalline metals. Sliding direction, $\langle 1\bar{1}0 \rangle$; sliding velocity, 3 mm/min; load, 0.05 to 0.3 N; room temperature; vacuum pressure, 10^{-8} Pa.

Figure 5. - Coefficients of friction as function of the actual shear strength of metals.

The actual shear strengths of metals were estimated from the experimental data of Bridgman (ref. 8). The shear phenomena and strength combined with high hydrostatic pressure were studied at pressures to a maximum of 4.9 gigapascals. The shear strength of the metal is very strongly dependent on the hydrostatic pressure acting on the specimen during the shearing process. The shear strength of the metal is increased with increasing applied hydrostatic pressure. The shear strength was estimated by extrapolation from contact pressure during sliding experiments by using the relations between the hydrostatic pressure and the shear strength obtained by Bridgman (refs. 18 and 8). The contact pressures for various metals in contact with nonmetals are calculated with Hertz's classical equations (ref. 19).

Figure 5 represents the friction properties of metals in contact with clean diamond, silicon carbide, and manganese-zinc ferrite as functions of the actual shear strength. The data of these figures indicate a decrease in friction with an increase of the actual shear strength of metal. There generally appears to be correlation between the friction and the actual shear strength of metal. This seems to indicate that the ratio of actual to ideal shear strength does not vary greatly from one elemental metal to another.

Summary of Results

The coefficients of friction for clean metals in contact with clean diamond, boron nitride, silicon carbide, manganese-zinc ferrite, and metals are generally related to the ideal and actual shear strength of metals. The higher strength of the metal, the lower the coefficient of friction. Coefficients of friction are also related to the shear modulus. Individually shear modulus, atomic size, and lattice constant also play important roles in adhesion and friction of solids.

Lewis Research Center
National Aeronautics and Space Administration
Cleveland, Ohio, March 12, 1981

References

1. Miyoshi, Kazuhisa; and Buckley, Donald H.: Friction and Wear Behavior of Single-Crystal Silicon Carbide in Sliding Contact with Various Metals. ASLE Trans., vol. 22, no. 3, July 1979, pp. 245-256.
2. Buckley, Donald H.: The Metal-to-Metal Interface and Its Effect on Adhesion and Friction. J. Colloid Interface Sci., vol. 58, no. 1, Jan. 1977, pp. 36-53.
3. Miyoshi, Kazuhisa; and Buckley, Donald H.: Adhesion and Friction of Single-Crystal Diamond in Contact with Transition Metals. Applications of Surface Science, 6 (1980), pp. 161-172.
4. Buckley, Donald H.: Friction and Transfer Behavior of Pyrolytic Boron Nitride in Contact with Various Metals. ASLE Trans., vol. 21, no. 2, Apr. 1978, pp. 118-124.
5. Miyoshi, Kazuhisa; and Buckley, Donald H.: Friction and Wear of Single-Crystal Manganese-Zinc Ferrite. Wear, vol. 66, pp. 157-173, 1981. Wear of Materials 1979, K. C. Ludema, W. A. Glaeser, and S. K. Rhee, eds., American Society of Mechanical Engineers, 1979, pp. 509-519. NASA TM-78980, 1979.

6. Miyoshi, Kazuhisa; and Buckley, Donald H.: The Relationship Between the Ideal Tensile Strength and Friction Properties of Metals in Contact with Nonmetals and Themselves. NASA TP E-587 (1980).
7. Macmillan, N. H.: Review: The Theoretical Strength of Solids. J. Mater. Sci. vol. 7, Feb. 1972, pp. 239–254.
8. Bridgman, P. W.: Shearing Phenomena at High Pressures, Particularly in Inorganic Compounds. Proc. Am. Acad. Arts Sci., vol. 71, 1937, pp. 387–460.
9. Polanyi, M.: Uber die Natur des ZerreiBvorganges. Z. Phys. vol. 7, 1921, pp. 323–327.
10. Orowan, E.: Mechanical Cohesion Properties and the "Real" Structure of Crystals. Z. Kristallog., vol. 89, no. 3–4, Oct. 1934, pp. 327–343.
11. Orowan, E.: Fracture and Strength of Solids. Rep. Prog. Phys., vol. 12, 1948–1949, pp. 185–232.
12. Orowan, E.: Energy Criteria of Fracture. Weld. J., vol. 34, Mar. 1955, pp. 157S–160S.
13. Frenkel, J.: Zur Theorie der Elastizitatsgrenze und der Festigkeit Kristallinischer Korper. Z. Phys., vol. 37, 1926, 572–609.
14. Gschneidner, Karl A., Jr.: Physical Properties and Interrelations of Metallic and Semimetallic Elements. Solid State Physics, Vol. 16, Frederick Seitz and David Turnbull, eds., Academic Press, 1964, pp. 275–426.
15. Barrett, Charles Sanborn: Structure of Metals, Crystallographic Methods, Principles, and Data, McGraw-Hill Book Co., Inc., 1943, pp. 552–554.
16. Lyman, Taylor: (editor): Metals Handbook Vol. 1: Properties and Selection of Metals, Eighth ed. American Society for Metals, 1961.
17. Tegart, William J. Mcgregor: Elements of Mechanical Metallurgy. Macmillan Co., 1966.

1. Report No.	2. Government Accession No.	3. Recipient's Catalog No.
NASA TP-1891		

4. Title and Subtitle
CORRELATION OF IDEAL AND ACTUAL SHEAR STRENGTHS OF METALS WITH THEIR FRICTION PROPERTIES

5. Report Date
July 1981

6. Performing Organization Code

7. Author(s)
Kazuhisa Miyoshi and Donald H. Buckley

8. Performing Organization Report No.
E-701

10. Work Unit No.

9. Performing Organization Name and Address
National Aeronautics and Space Administration
Lewis Research Center
Cleveland, Ohio 44135

11. Contract or Grant No.

13. Type of Report and Period Covered
Technical Paper

12. Sponsoring Agency Name and Address
National Aeronautics and Space Administration
Washington, D. C. 20546

14. Sponsoring Agency Code

15. Supplementary Notes

16. Abstract

The relation between the ideal and actual shear strengths and friction properties of clean metals in contact with clean diamond, boron nitride, silicon carbide, manganese-zinc ferrite and the metals themselves in vacuum is discussed. An estimate of the ideal shear strength for metals is obtained from the shear modulus, the repeat distance of atoms in the direction of shear of the metal and the interplanar spacing of the shearing planes. The coefficient of friction for metals is shown to be correlated with both the ideal and actual shear strength of metals. The higher the strength of the metal, the lower the coefficient of friction.

17. Key Words (Suggested by Author(s))	18. Distribution Statement
Tribology Shear strength	Unclassified - unlimited STAR Category 27

19. Security Classif. (of this report)	20. Security Classif. (of this page)	21. No. of Pages	22. Price*
Unclassified	Unclassified	11	A02

* For sale by the National Technical Information Service, Springfield, Virginia 22161

NASA-Langley, 1981

3 1 1U,C, 071081 S00903DS
DEPT OF THE AIR FORCE
AF WEAPONS LABORATORY
ATTN: TECHNICAL LIBRARY (SUL)
KIRTLAND AFB NM 87117